

# Experimentally quantifying critical stresses associated with basal and prismatic slips in Zn and Zn-Ag alloys using *in situ* micropillars compression

Maria Wątroba<sup>1</sup>, W. Bednarczyk<sup>2</sup>, M. Jain<sup>1,3</sup>, K. Wiecezrak<sup>1</sup>, J. Schwiedrzik<sup>1</sup>, P. Bała<sup>4</sup>, J. Michler<sup>1</sup>

<sup>1</sup> Empa, Swiss Federal Laboratories for Materials Science and Technology, Thun, Switzerland  
<sup>2</sup> Warsaw University of Technology, Warsaw, Poland  
<sup>3</sup> University of New South Wales, Sydney NSW 2052, Australia  
<sup>4</sup> AGH University of Science and Technology, Krakow, Poland



Materials Science and Technology

## MOTIVATION & OBJECTIVES

- \* **Zinc** (Zn) has been considered a novel promising material for bioresorbable medical implants.
- \* **Poor strength and brittleness** of as-cast **pure Zn** require **alloying with other elements** and **plastic deformation** for grain size refinement to enhance mechanical properties (Fig. 1).

\* Mechanical properties testing:

- **in the macroscale**
- The strengthening effect is affected by:
  - ▶ grain size;
  - ▶ texture;
  - ▶ phase composition;
  - ▶ fraction and type of GBs;
  - ▶ deformation mechanisms.

- **in the microscale**
- Individual strengthening effect can be distinguished:
  - ▶ size effect;
  - ▶ solid solution strengthening.
- Besides, one deformation mechanism can be activated within a single grain, so critical resolved shear stresses in a specific slip system can be measured.

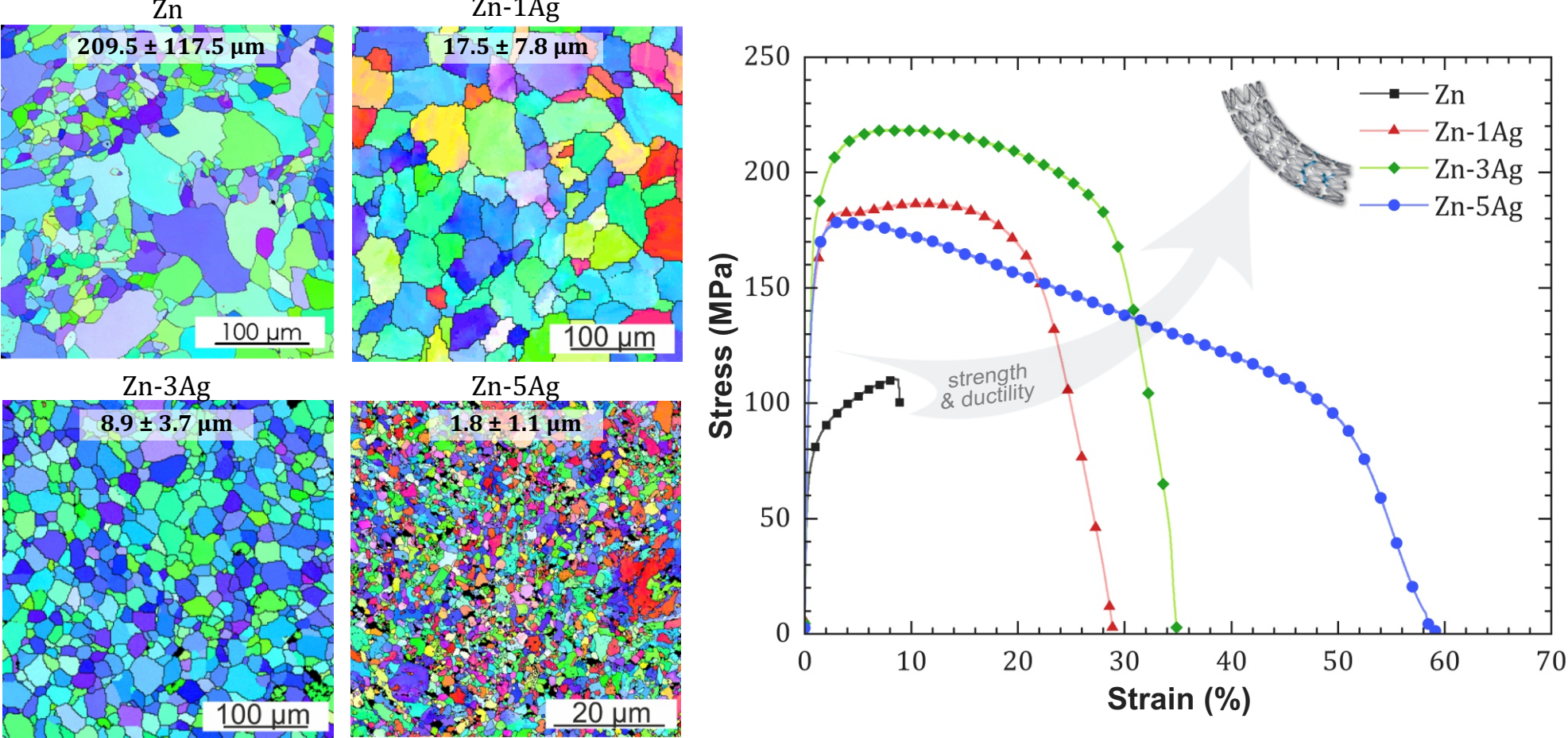


Fig. 1. Effect of Ag additions and hot extrusion on the microstructure and mechanical properties of Zn alloys

## MICROPILLARS FABRICATION

- \* The samples of the **Zn-xAg** alloys ( $x = 0 \div 2.21$  at.%) were fabricated by casting and annealing.
- \* Grains with the highest Schmid Factor for **basal and prismatic slip system** were selected for the micropillars fabrication.

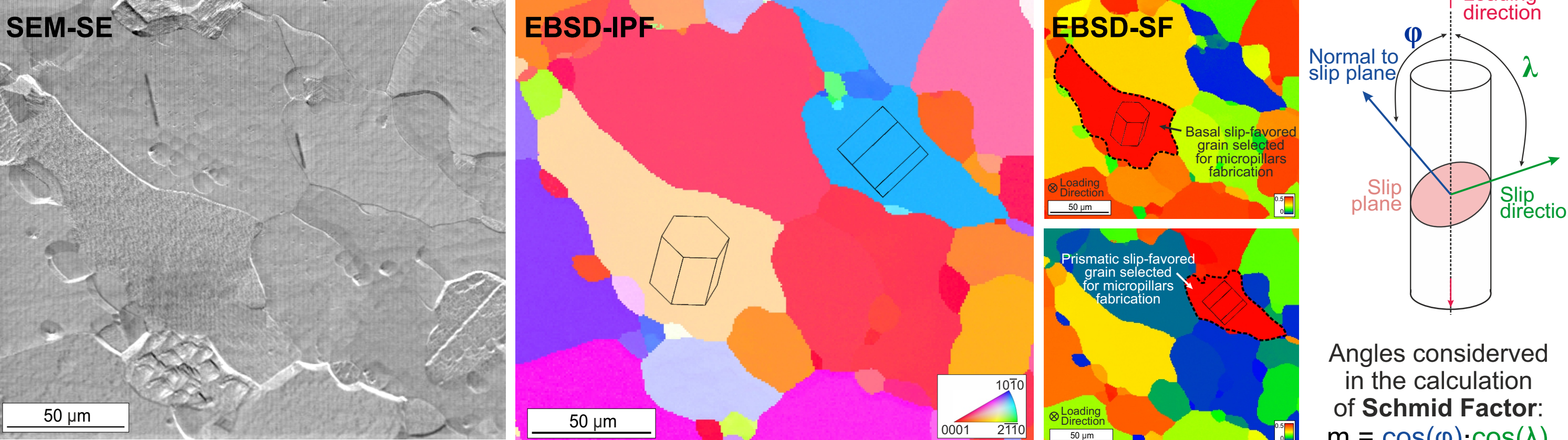


Fig. 2. Microstructure of the annealed sample; EBSD-IPF orientation map; SF maps for basal and prismatic slip system; angles considered in the calculation of the Schmid factor.

- \* Micropillars were fabricated by multi-step Ga<sup>+</sup> focused ion beam (FIB) milling operated at 30kV and beam currents from 4.5 nA to 40 pA.
- \* A micropillar **diameter** between **3 μm** and **9 μm** had been chosen based on the studies [1-2]: **transition from twinning to dislocation slip** dominant deformation mechanism occurred within this grain size range.

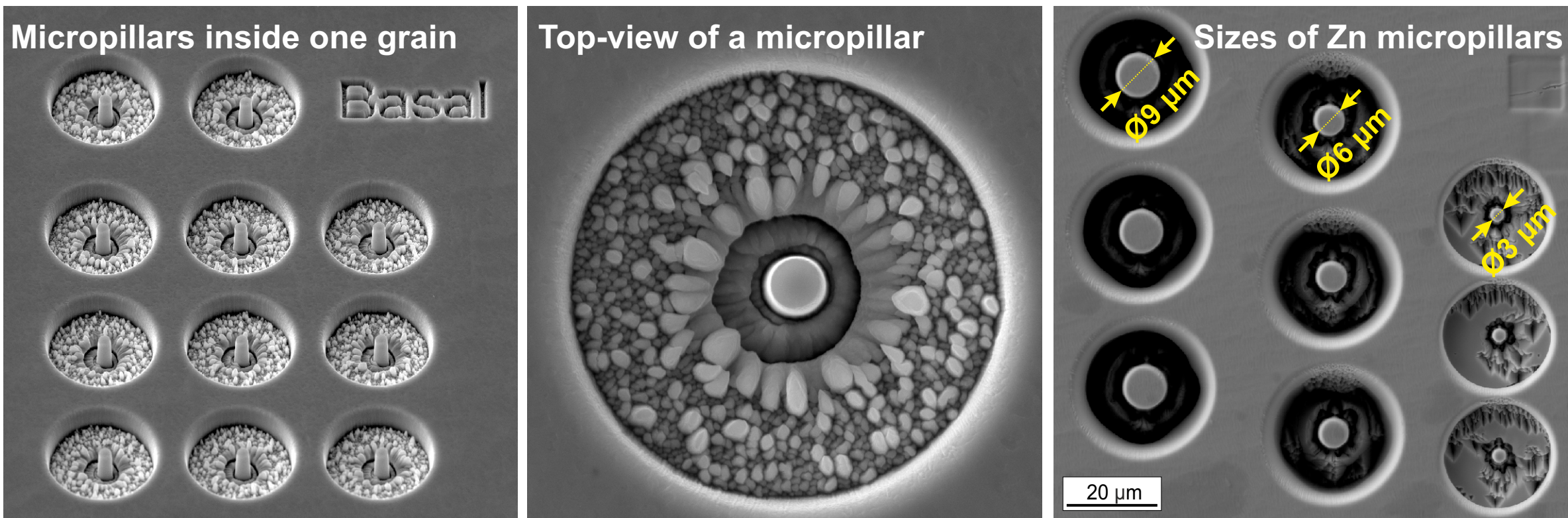


Fig. 3. Micropillars prepared for the compression tests with single grain with basal- or prismatic- slip favoured orientation

## IN SITU MICROPILLARS COMPRESSION

- \* Micropillars compression tests were performed using flat punch installed in Alemnis Standard Assembly **in situ nanoindentation system** (Fig. 4) up to ~10% of deformation
- \* Different-sized **pure Zn** micropillars were deformed at  $10^3$  s<sup>-1</sup> to investigate the **size effect on CRSS**
- \* **Zn-xAg** micropillars (ø3 μm) were deformed at  $10^4$ ,  $10^3$ ,  $10^2$  s<sup>-1</sup> to measure the effect of Ag on CRSS
- \* According to the **Schmid Law**, CRSS can be calculated based on the yield stress ( $\sigma_{0.2}$ ) determined from the stress-strain curves and Schmid Factor ( $m$ ) calculated for a single grain and particular slip system

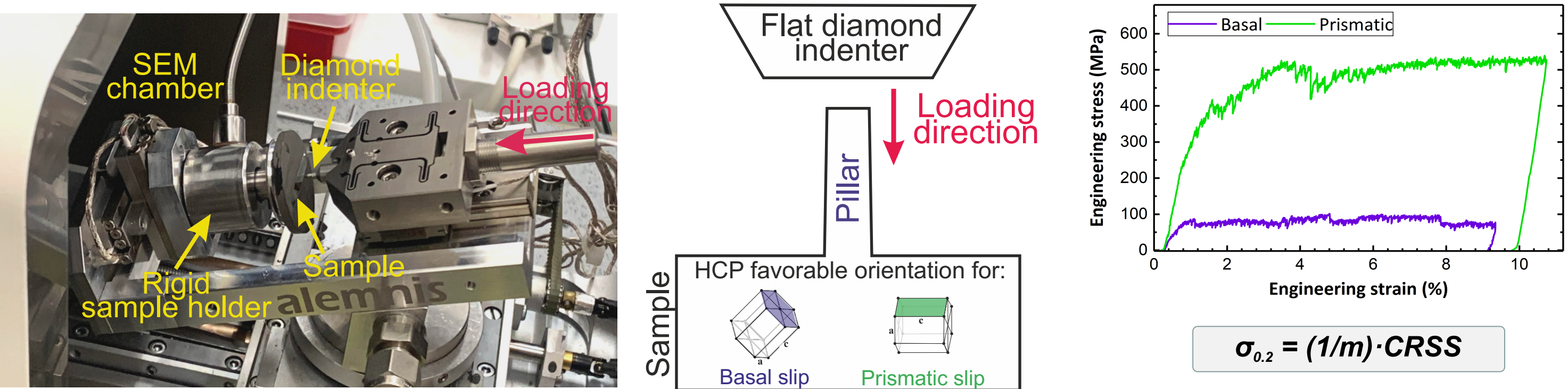


Fig. 4. Setup for the in situ micropillars compression and the example of stress-strain curves

## FUTURE PERSPECTIVES

- ▶ Current studies provide fundamental knowledge about possibilities of Zn solid solution strengthening.
- ▶ Calculated CRSS can be further implemented in crystal plasticity models, as input data, for designing fabrication processes of bioresorbable implants requiring specific mechanical properties.
- ▶ Investigated here Zn-Ag system can be used as an antibacterial thin coating on the biomedical devices, such as orthopedic implants.
- ▶ The knowledge gained in this research will be translated into the design of novel Zn-based porous metamaterials with tailored microstructure and tunable properties for potential bioresorbable maxillofacial implant applications.

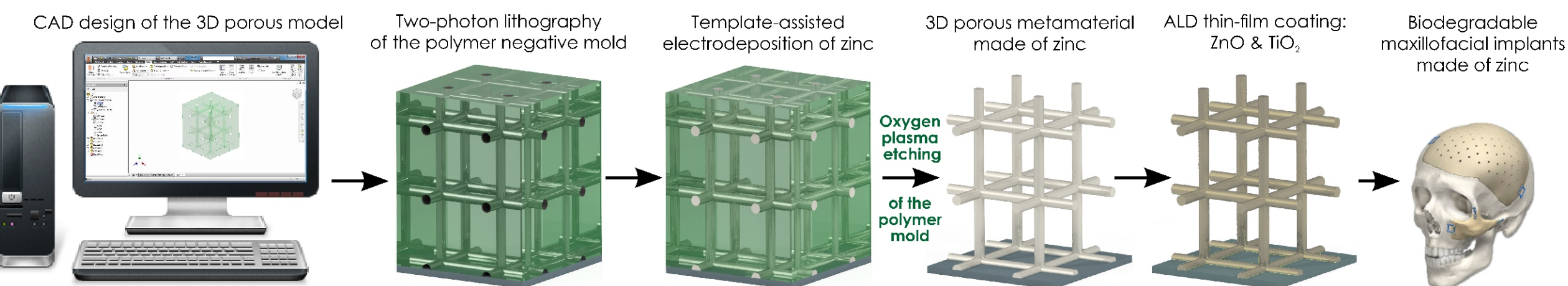


Fig. 5. Process diagram for fabrication of coated Zn-based metamaterials

## SIZE EFFECT IN PURE Zn

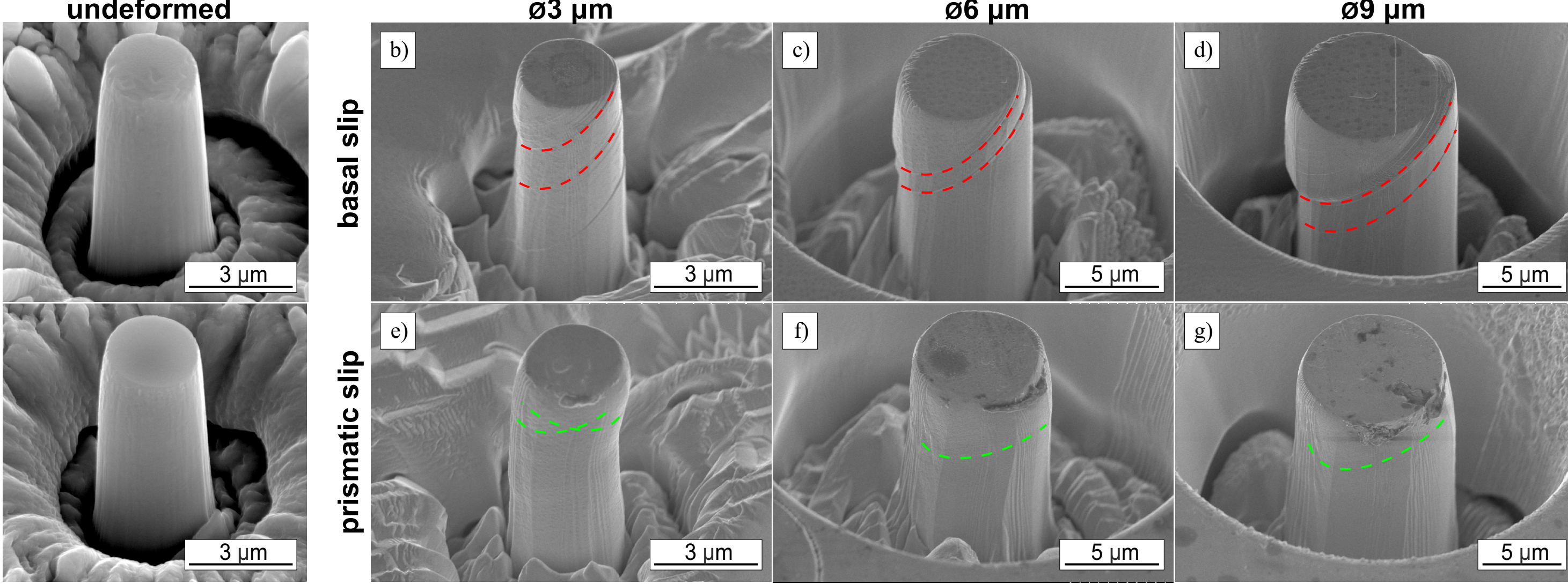


Fig. 6. SEM images of undeformed and deformed micropillars in basal and prismatic slip system;

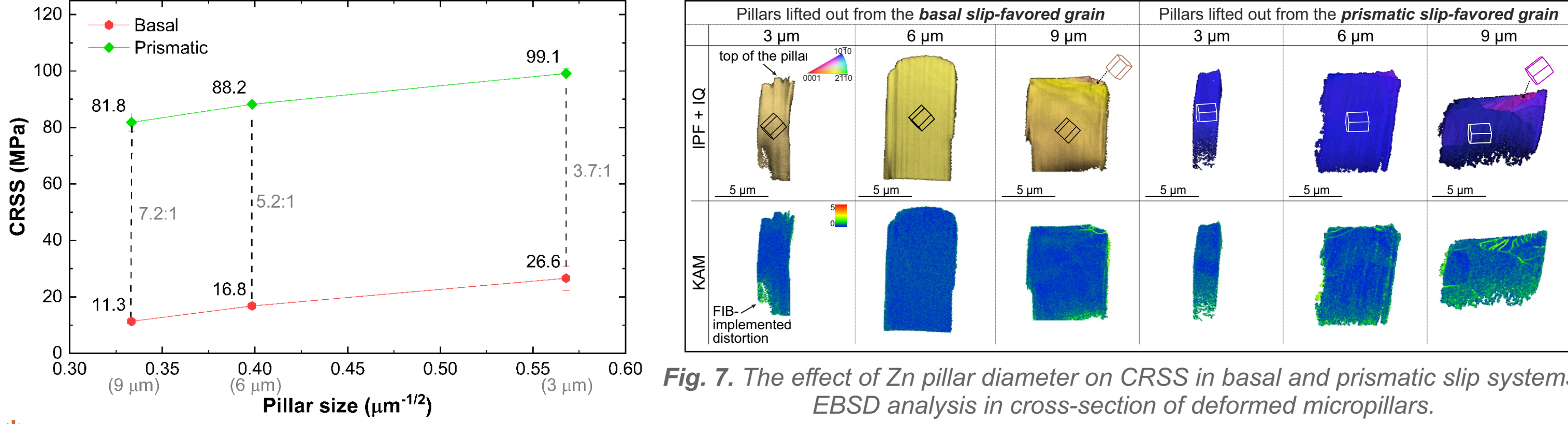


Fig. 7. The effect of Zn pillar diameter on CRSS in basal and prismatic slip systems. EBSD analysis in cross-section of deformed micropillars.

- \* A significant **yield stress and CRSS increase** with the micropillar **diameter reduction** was observed.
- \* The deformation in the **basal slip** system produced **slip traces, distinctly separated in 3 μm** pillars and **localized for 9 μm** pillars.
- \* **Prismatic slip traces on two slip planes** were observed in **3 μm** pillars and **only one** can be seen in **6 μm** and **9 μm** pillars.
- \* A **uniform orientation within 3 μm** pillars deformed up to 10% was observed, while in **bigger pillars** a **localized deformation** occurred on the top of the pillar, resulting in a lattice rotation.

## SOLID SOLUTION EFFECT IN Zn - xAg ALLOYS

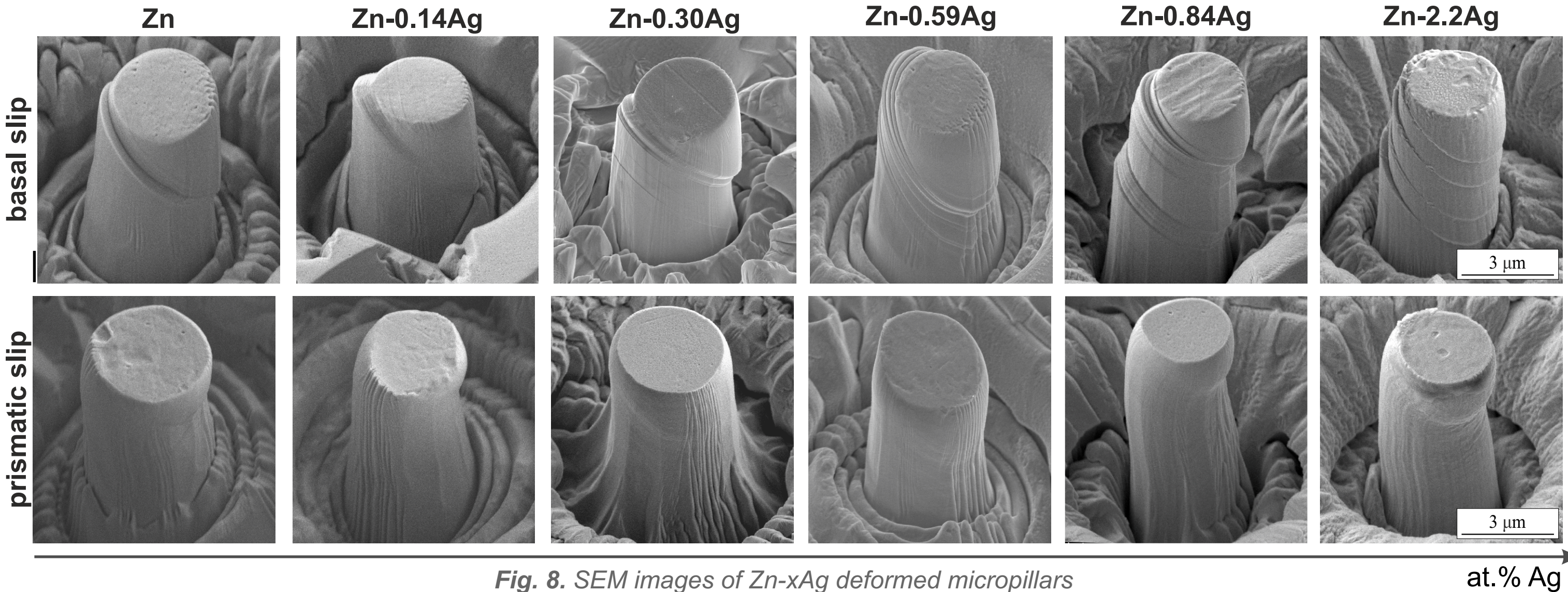


Fig. 8. SEM images of Zn-xAg deformed micropillars

- \* Ag content is increasing →
- \* the recrystallization at RT is suppressing →
- \* dislocation density is increasing →
- \* the probability of finding dislocation source is increasing →
- \* Change in basal slip character from localized deformation in pure Zn to uniform in the Zn-2.2Ag alloy. Prismatic slip takes place in two favorable planes resulting in buckling than localized pure shearing.

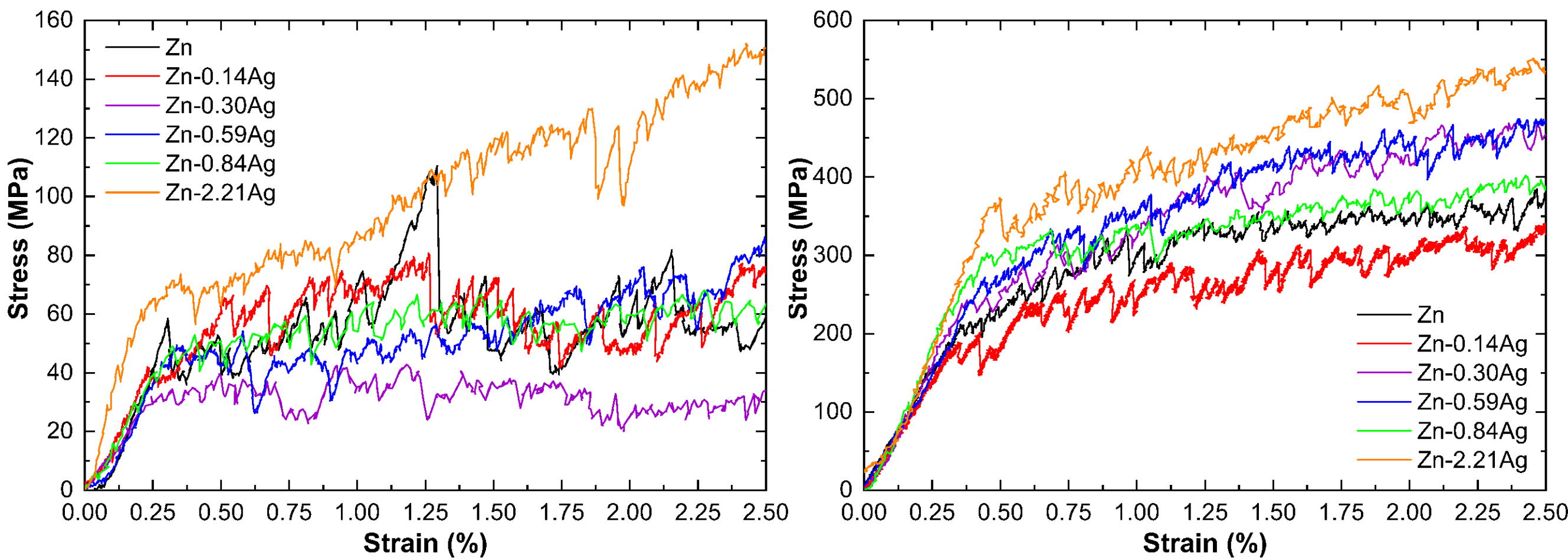


Fig. 9. Compression stress-strain curves of pure Zn and Zn-Ag alloys

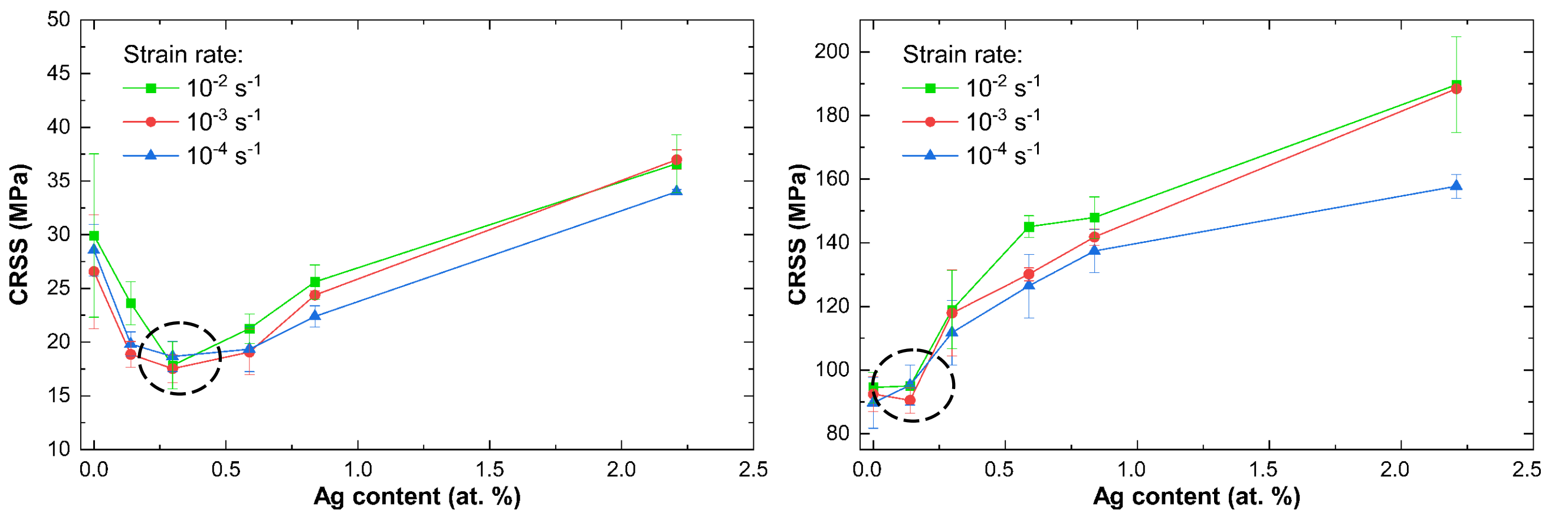


Fig. 10. The effect of Ag content on CRSS in basal and prismatic slip systems at various strain rates

- \* **Strain rate sensitivity:** **no** significant **effect in basal slip system**, while in **prismatic slip system**, pronounced **effect** was seen **above 0.59 at. % Ag**.
- \* **Strengthening effect:** **small Ag** additions result in **decrease** of both **CRSS<sub>b</sub>** (up to 0.3 at. % Ag) and **CRSS<sub>p</sub>** (up to 0.14 at. % Ag) while **further increase in Ag** content, **increase the CRSS** in both cases.
- \* According to [3] initial drop and further increase of CRSS with Ag additions result from increasing dislocation density in the micropillars. The transition in strengthening source is expected as follows: dislocation starvation → single-source strengthening → exhausted hardening → forest hardening.

### References:

- [1] M. Wątroba, et al., Fine-tuning of mechanical properties in a Zn-Ag-Mg alloy via cold plastic deformation process and post-deformation annealing, Bioact. Mater. 6 (2021) 3424–3436.
- [2] W. Bednarczyk, M. Wątroba, et al., Abnormal grain growth in a Zn-0.8Ag alloy after processing by high-pressure torsion, Acta Mater. 207 (2021) 116667.
- [3] J.A. El-Awady, Unravelling the physics of size-dependent dislocation-mediated plasticity, Nat. Commun. 6 (2015) 5926.